JOURNAL OF ENERGY, MATERIALS, AND INSTRUMENTATION TECHNOLOGY

Journal Webpage https://jemit.fmipa.unila.ac.id/

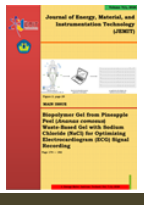

Monte Carlo Simulation of Dose Distribution in Prostate Cancer of Boron Neutron Capture Therapy (BNCT) Using PHITS v.3.35

Muhammad Nashrun Basyaruddin[1], Raditya Faradina Pratiwi[1*], Yohannes Sardjono[2], Gede Sutrisna Wijaya[2] ,Isman Mulyadi Triatmoko[2], Fendinugroho[2], Nunung Nuraeni[2], and Heru Prasetio[2]

1. Department of Physics, Faculty of Mathematics and Natural Sciences, Defense University, IPSC Sentul Bogor, Indonesia
2. Research Center for Safety, Meteorology and Nuclear Quality Technology, Research Organization for Nuclear Energy, National Research and Innovation Agency, Indonesia

Article Information

Article history:
Received November 3, 2025
Received in revised form February 27, 2026
Accepted February 28, 2026

Keywords: *BNCT,Prostate Cancer , PHITS, Monte Carlo Simulation, Dosimetry*

Abstract

Prostate cancer is the fifth leading cause of cancer death in men worldwide. With its ability to selectively kill tumor cells, Boron Neutron Capture Therapy (BNCT) has reemerged as a promising radiation therapy option for treating prostate cancer. This therapy is known for delivering high doses directly to the target while minimizing damage to healthy tissue. This study aims to analyze the absorbed dose and irradiation time in prostate cancer BNCT under different beam angles using the Particle and Heavy Ion Transport code System (PHITS) v3.35 A computational phantom based on the ORNL adult male model was constructed, incorporating a prostate tumor with a diameter of 1.277 cm to represent a localized lesion. The neutron source was modeled as a 30 MeV proton accelerator and boron concentrations of 84, 104, and 124 μg/g were applied to evaluate their influence on total dose rate and treatment duration at irradiation angles of 0°, 30°, and 60. Results indicate that higher boron concentration significantly reduces irradiation time while maintaining organ-at-risk (OAR) doses below 5 Gy. The optimal configuration was achieved at 0° with a boron concentration of 124 μg/g, resulting in a total irradiation time of 30.59 minutes and a tumor equivalent dose of ~76 Gy. These findings confirm the feasibility of PHITS-based Monte Carlo modeling for optimizing BNCT treatment planning in prostate cancer.

Informasi Artikel

Proses artikel:
Diterima 3 November 2025
Diterima dan direvisi dari 27 Februari 2026
Accepted 28 Februari 2026

Kata kunci: *BNCT, Kanker Prostat, PHITS, Simulasi Monte Carlo, Dosimetri*

Abstrak

Kanker prostat adalah penyebab kematian kanker kelima terbanyak pada pria di seluruh dunia. Dengan kemampuannya untuk secara selektif membunuh sel tumor, Terapi Penangkapan Neutron Boron (BNCT) telah muncul kembali sebagai opsi terapi radiasi yang menjanjikan untuk pengobatan kanker prostat. Terapi ini dikenal karena kemampuannya memberikan dosis tinggi langsung ke target sambil meminimalkan kerusakan pada jaringan sehat. Penelitian ini bertujuan untuk menganalisis dosis yang diserap dan waktu iradiasi pada BNCT kanker prostat dengan sudut berkas yang berbeda menggunakan Particle and Heavy Ion Transport code System (PHITS) v3.35. Phantom komputasi berdasarkan model pria dewasa ORNL dibangun, dengan memasukkan tumor prostat berdiameter 1,277 cm untuk mewakili lesi yang terlokalisasi. Sumber neutron dimodelkan sebagai akselerator proton 30 MeV, dan konsentrasi boron 84, 104, dan 124 μg/g diterapkan untuk mengevaluasi pengaruhnya terhadap laju dosis total dan durasi pengobatan pada sudut iradiasi 0°, 30°, dan 60°. Hasil menunjukkan bahwa konsentrasi boron yang lebih tinggi secara signifikan mengurangi waktu iradiasi sambil menjaga dosis organ yang berisiko (OAR) di bawah 5 Gy. Konfigurasi optimal tercapai pada sudut 0° dengan konsentrasi boron 124 μg/g, menghasilkan waktu iradiasi total sebesar 30,59 menit dan dosis ekuivalen tumor sekitar 76 Gy. Temuan ini mengonfirmasi kelayakan pemodelan Monte Carlo berbasis PHITS untuk mengoptimalkan perencanaan pengobatan BNCT pada kanker prostat.

* Corresponding author.
E-mail address: radityafaradina@gmail.com

1. Introduction

Prostate cancer is the fifth leading cause of cancer death in men worldwide, with 1,276,106 new cases and 358,989 deaths each year (Jain & Sapra, 2020). In 2022, Indonesia recorded 408,661 new cases and 242,988 deaths from prostate cancer, ranking fifth in terms of new cases and seventh in terms of deaths. Prostate cancer occurs in men and can be caused by age, ethnicity, and family history, but there are other environmental factors that play an important role in tumor formation (International Agency for Research on Cancer, 2022; Sung et al., 2020; Arigbede et al., 2024).

The prostate is a male sexual gland that is shaped and sized similarly to a walnut. It is located in the lower pelvis, just below the bladder and in front of the rectum (Lee et al., 2011). Prostate cancer generally develops in the prostate gland, which is located below the bladder in men, specifically around the urethra, which is the tube that carries urine from the bladder out of the body. The prostate gland functions to produce fluid that is part of semen. Tumors in prostate cancer often start in the outer part of the prostate gland (W. Bolland, 2008). Using biparametric magnetic resonance imaging (bpMRI) is now recognized as the gold standard in imaging for diagnosis, staging, and gross tumor volume (GTV) planning in prostate cancer (PCa) (Panebianco et al., 2018). In the development of radiotherapy, several new methods such as Boron Neutron Capture Therapy (BNCT), Proton Beam Therapy, Fast Neutron Therapy, X-ray Therapy, and Carbon Ion Therapy are being tested. However, among the developments in radiotherapy, BNCT is the most promising, thanks to its ability to reduce damage to healthy tissue not affected by the tumor (Purohit & Kumar, 2022). The BNCT treatment mechanism is demonstrated in **Figure 1**.

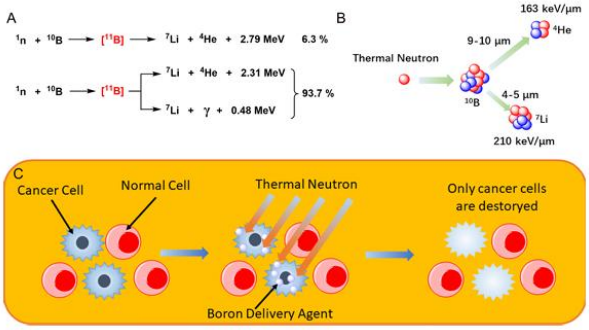

Figure 1. (A) Boron atomic nuclear reactions, the dominant ones of which are accompanied by the production of high-energy rays. (B) Boron Neutron Capture Therapy (BNCT) mechanism. (C) Schematic diagram of BNCT, which selectively kills tumor cells (Wang et al., 2022).

BNCT is based on the capture and fusion reactions that occur when non-radioactive ^{11}B is irradiated with low-energy thermal neutrons to produce ^{11}B, which then undergoes an instantaneous nuclear reaction to produce high-energy α particles and high-energy ^{7}Li (Jin et al., 2022). The particles focus on the directed release of high-LET linear energy transfer particles within cancerous tissue after boron ^{10}B captures neutrons (Koivunoro et al., 2019). The advantage of BNCT over other radiotherapy methods is its ability to selectively irradiate cancer cells. With just one irradiation session, BNCT can deliver an effective high dose to the tumor area while reducing exposure to healthy tissue ("Boron Neutron Capture Therapy: Cellular Targeting of High Linear Energy Transfer Radiation", n.d.). In comparison, proton therapy and carbon ion therapy, which rely on the Bragg peak, expose normal tissue to a significant dose of radiation before reaching the tumor, as shown in figure 2. In addition, the dose is received by normal tissue surrounding the tumor. However, BNCT delivers a much lower dose to healthy tissue, unlike cancer cells.

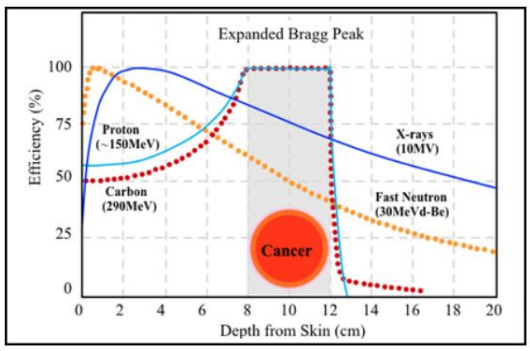

Figure 2. Effectiveness of BNCT (source: http://www.jsnct.jp)

All BSA have a cylindrical structure with a beryllium target and a beam channel located on the central axis of the cylinder. The main role of this process is to moderate the energy of neutrons produced by protons so that they reach the thermal or epithermal neutron energy range, without producing excessive gamma rays. Another equally important part is the reflector, which serves to reflect scattered neutrons back into the neutron flow. BSA can convert the proton beams produced by the cyclotron into neutrons through interactions between protons and the target, such as lithium or beryllium (Li et al., 2021). In BNCT, the dose consists of four components, namely alpha, boron, neutron, and proton doses. Each component must meet certain requirements, whereby the boron dose must be appropriate for the depth of the tumor. When calculated using Excel and plotted on a graph, it can be seen that the boron dose rises and is higher than the other doses (Fukuda, 2021).

Previous studies on prostate BNCT primarily investigated anterior–posterior beam directions without considering angular variations that could influence dose uniformity and organ-at-risk (OAR) exposure (Ogawa, et al., 2024; Meher et al., 2021). Beam angle optimization is critical for minimizing neutron attenuation and improving dose conformity, particularly for deep-seated targets such as the prostate gland. However, only limited computational analyses have addressed multi-angle irradiation in prostate BNCT using the latest PHITS version, which incorporates updated nuclear data libraries and advanced dose-scoring algorithms. Several Monte Carlo studies using standard ICRP phantoms have shown that tumor depth strongly influences the absorbed dose, with shallower targets receiving higher energy deposition while doses to surrounding tissues remain relatively constant (Mirzaei et al., 2014). Additionally, the application of lithium filters has been proven effective in reducing neutron leakage and protecting normal tissue from overexposure (Mirzaei et al., 2014).

2. Methodology

2.1 Computational Setup

Monte Carlo simulations were performed using the Particle and Heavy Ion Transport code System (PHITS) version 3.35. The simulation utilized the JENDL-4.0 and ENDF/B-VII.1 nuclear data libraries for precise neutron interaction modeling. The patient simulation geometry consisted of the ORNL adult male phantom, as well as body composition data taken from Report 145 of the International Commission on Radiological Protection (ICRP) (Yeom *et al.*, 2019; Krstic et al., 2014).

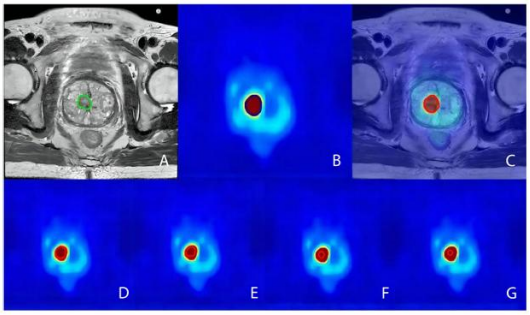

Figure 3. A 70-year-old male with prostate cancer in the 18F subgroup. The green line represents GTV-MRI (A). The blue line represents GTV-PET (B). The red line represents GTV-PET/MRI (C) (Zhang et al., 2022)

A case in figure 3. 70-year-old man from subgroup 18F underwent examination with the 18F-PSMA-1007 tracer using a PET/MRI system, which combines metabolic and anatomical information (T1WI, T2WI, DWI). PET/MRI demonstrated high accuracy in GTV delineation and has significant potential to support radiotherapy planning in prostate cancer (Zhang et al., 2022). A spherical prostate tumor was modeled with a diameter of 1.277 cm. To ensure statistical precision, 10^8 neutron histories were used, maintaining uncertainty below 1–2%.

Table 1. Description parameter

Simulation Parameter	Value/ Description	Refrence/ Note
Simulation code	PHITS v3.35	JAEA,Japan
Neutron source	30MeV proton accelerator (cyclotron-based)	(Jagt et al., 2024)
Target material	Beryllium (Be)	BSA configuration
Phantom	ORNL adult male	ICRP Report 145
Tumor Geometry	Spherical, 1.277cm diameter	This Work
Boron concentration	84,104,124 µg/g	Variable
Neutron flux (φ_epi)	1.13 x 10^9 n/cm^2-s	IAEA-complaint
Number of particle histories	1x10^8	-
Tally type	Dose & flux scoring	F6 & T-Track in PHITS

The prostate, bladder, rectum, and surrounding soft tissues were explicitly modeled to evaluate Organ-at-Risk (OAR) doses. The simulation was performed using 10^8 neutron histories to ensure sufficient statistical precision. The statistical uncertainty for each tally was maintained below 1-2% (Jagt et al., 2024).

2.2 Neutron Source and Beam Sharping Assembly (BSA)

The neutron source was modeled to represent a cyclotron-based 30 MeV proton beam with a current of 1 mA striking a beryllium target, following the configuration of the HM-30 accelerator developed by Sumitomo Heavy Industries (Nakamura et al., 2022). Cyclotrons have proven to be safe and effective accelerators as neutron sources for BNCT. Compared to other accelerators such as LINACs and electrostatic accelerators, cyclotrons provide a very stable beam. This is because cyclotrons can generate a continuous beam with high intensity, which is a significant advantage in proton beam distribution (Kumada et al., 2023; Lu et al., 2023). The BSA collimator illustration in

Figure 4 in this study is the result of replicating the optimization process previously conducted by I Made Ardhana (Ardana & Sardjono, 2017). A BSA collimator is designed to produce IAEA-compliant neutron flux so that it can be used in BNCT therapy and its components are listed in **Table 2**.

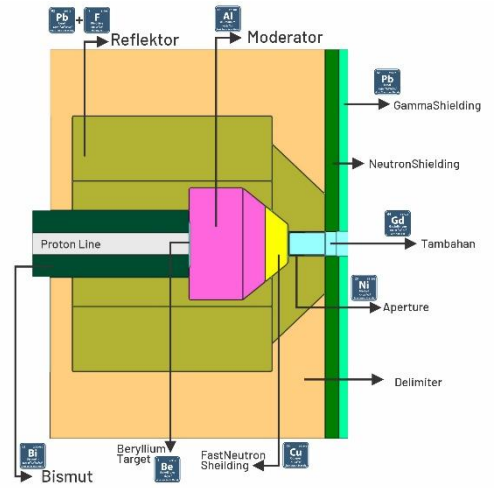

Figure 4. BSA collimator design (Ardana & Sardjono, 2017)

Table 2. Names of BSA components and materials

No	Names Components	Material	Function
1	Target	*Be*	Proton-neutron conversion
2	Reflector	*PbF2*	Neutron Backscattering
3	Moderator	*Al*	Energy Reduction
4	Fast Neutron Filter	*Copper*	Reduce the intensity of fast neutrons
5	Neutron Thermal Filter	*Gd*	To absorb thermal neutrons
6	Aperture	*Ni*	Control the flow and direction of neutrons
7	Bismuth	*Bi*	Used for radiation shielding
8	Gamma Shielding	*Pb*	Gamma shielding
9	Delimiter	*Lithiated Polyethylene*	To act as a barrier or protector
10	Neutron Shielding	*Boroted Paraffin Wax*	Neutron shielding
11	Additional	*Gd*	Additional material for neutron absorption

The optimized BSA configuration produced an epithermal neutron flux of 1.13×10^{9} n/cm²·s, with gamma and fast neutron dose rates well within IAEA BNCT beam quality recommendations.

2.3 Irradiation Geometry

To evaluate the impact of beam direction on dose distribution, three irradiation angles relative to the phantom axis were modeled: 0°, 30°, and 60°.

- 0° irradiation: beam aligned along the central body axis (anterior–posterior).
- 30° irradiation: beam incident obliquely to the right lateral side.
- 60° irradiation: beam incident more tangentially toward the pelvic region.

The prostate tumor was centered within the beam field for all cases. The neutron source-to-surface distance (SSD) was maintained constant at 100 cm. **Figures 5a-c** illustrate the irradiation geometry in axial sections for each configuration.

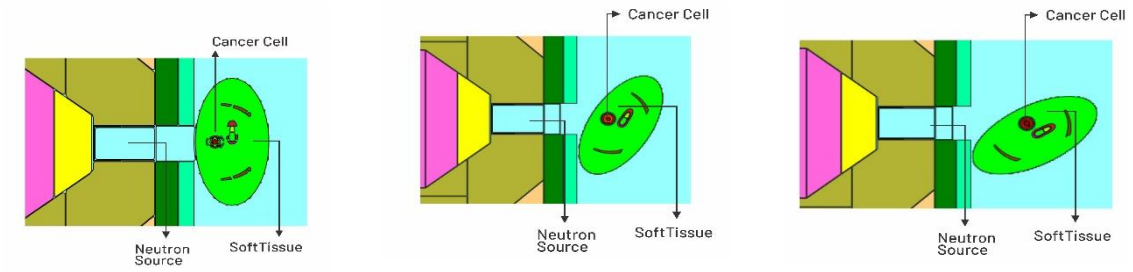

(a) (b) (c)

Figure 5. Visualization of irradiation direction in the axial (a) 0˚, (b) 30˚, (c) 60˚

2.4 Dose Component and Calculation

The BNCT core reaction involves four main factors to be considered: gamma dose, boron dose, neutron dose, and proton dose. The dose rate values for these components are derived from the PHITS program output and processed in Microsoft Excel to calculate the total dose, irradiation time, and equivalent dose.

The total absorbed dose rate ($\dot{D}_T$) in BNCT consists of fourmain components (Li et al., 2021a):

$$\dot{D}_T = \left(w_b \, x \, \dot{D}_B\right) + \left(w_p \, x \, \dot{D}_p\right) + \left(w_n \, x \, \dot{D}_n\right) + \left(w_\gamma \, x \, \dot{D}_\gamma\right) \quad (1)$$

where,

$\dot{D}_T$ = total dose rate (Gy/s)
w_b = boron weight factor
w_p = nitrogen weight factor
w_n = neutron weight factor fast
w_γ = photon weight factor

To determine the irradiation time, the total dose to the GTV must first be calculated. The irradiation time is calculated by dividing the minimum dose required for cancer destruction by the total dose rate to the GTV. The irradiation time (t) required to reach the minimum therapeutic dose ($D_{\min}$ = 76 Gy), intermediate-risk group (Li et al., 2021b) is:

$$t = \frac{D_{minimum}}{D_{T\,GTV}} \quad (2)$$

After irradiation, the total equivalent dose (D_T) in BNCT is calculated by summing the four main dose components, each multiplied by its respective biological weighting factor. Based on IAEA and clinical BNCT literature, the following weighting factors (ω) were applied to convert physical dose (Gy) to equivalent dose (Gy-Eq):

Table 3. Dose Components and Applied Weighting Factors (ω)

Dose Component	Weighting Factor (ω)	Reference / Source	Note
Boron Dose ($\dot{D}_B$)	3.8 (Tumor) 1.3 (Healthy)	(Koivunoro et al., 2019; Schwint et al., 2020)	Compound Biological Effectiveness (CBE)
Nitrogen Dose ($\dot{D}_p$)	3.2		Due to $N^{14}(n,p)C^{14}$ reaction
Fast Neutron Fast ($\dot{D}_n$)	3.2		Relative Biological Effectiveness (RBE)
Gamma Dose ($\dot{D}_\gamma$)	1.0		Low Linear Energy Transfer (LET) radiation

$$D = \dot{D}_T \times t \quad (3)$$

PHITS software was used to calculate the dose and exposure in BNCT, with the results being determined for different boron concentration variations of 84 µg/g, 104 µg/g, and 124 µg/g.

2.5 Treatment Plant Evaluation

To evaluate the precision of the dose distribution relative to the target volume, a Conformity Analysis was performed. The Conformity Index (CI) was calculated using the following equation (Feuvret et al., 2006):

$$CI = \frac{D_{minimum}}{TV} \quad (4)$$

where $D_{minimum}$ is the minimum therapeutic dose (76 Gy) and TV is the target volume (GTV) of 1.09 cm³. A CI value closer to 1.0 indicates that the radiation dose is highly conformed to the tumor shape, minimizing exposure to surrounding healthy tissues.

2.6 Validation and Uncertainty

Validation was performed by comparing the calculated neutron flux and dose components in a water phantom against the IAEA BNCT beam quality guidelines and the benchmark. The simulated epithermal flux (1.13×10^9 n/cm²·s) deviated by less than 5% from reference data, confirming the model's reliability. The relative statistical uncertainty per voxel was ≤3%, satisfying Monte Carlo precision standards. Systematic uncertainty from boron uptake ratio (10:5:1 for GTV:CTV:healthy tissue) was assessed through sensitivity analysis.

Table 4. BSA output results with water phantom

Parameter	IAEA Recommendations	Result
Ephithermal Neutron Flux (n/cm^2s)	>$1.0x10^9$	$1.13x10^9$
FastNeutron DoseRate/Ephithermal Neutron Flux ($Gycm^2/n$)	<$2.0x10^{-13}$	$6.35x10^{-14}$
Gamma DoseRate/Ephithermal Neutron Flux ($Gycm^2/s$)	<$2.0x10^{-13}$	$8.35x10^{-14}$
The Ratio of Thermal and Ephithermal NeutronFlux ($\varphi th/\varphi_{ephi}$)	<0.05	0.0252
The Ratio of Neutron Current and Neutron Flux (J/φ_{ephi})	>0.7	0.785

2.7 Workflow

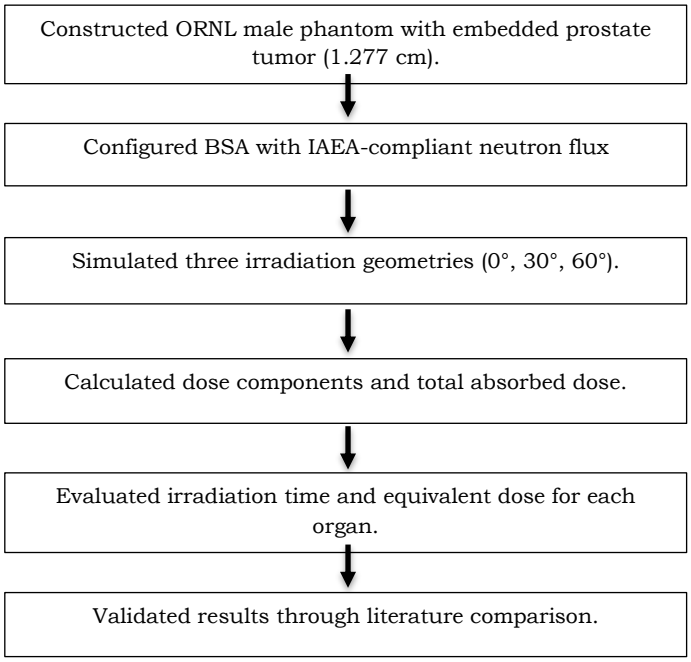

Figure 6. Workflow of Monte Carlo simulation using PHITS v3.35 for BNCT dose analysis in prostate cancer

3. results and discussion

3.1 Spatial Dose Distribution

Figure 5 shows the axial dose maps for irradiation angles of 0°, 30°, and 60° obtained from PHITS simulations. The highest dose concentration was observed in the prostate region, with a rapid dose fall-off toward the bladder and rectum. At 0° irradiation, the dose distribution was symmetrical and well-confined around the target, indicating optimal beam alignment along the central body axis.

In contrast, the 30° and 60° beam angles exhibited a more elongated pattern due to lateral neutron scattering and attenuation through surrounding tissues. The increased path length in soft tissue caused a reduction in neutron energy before reaching the tumor, leading to lower absorbed dose rates and less uniform contours. These results suggest that beam incidence plays an essential role in achieving dose conformity in prostate BNCT.

3.2 Effect of Boron Concentration on Dose Rate Distribution

The total absorbed dose rate in the *gross tumor volume* (GTV) increased significantly with boron concentration. This relationship is governed by the reaction probability of the $^{10}B(n,\alpha)^7Li$ process, which is proportional to boron atom density in the tissue.

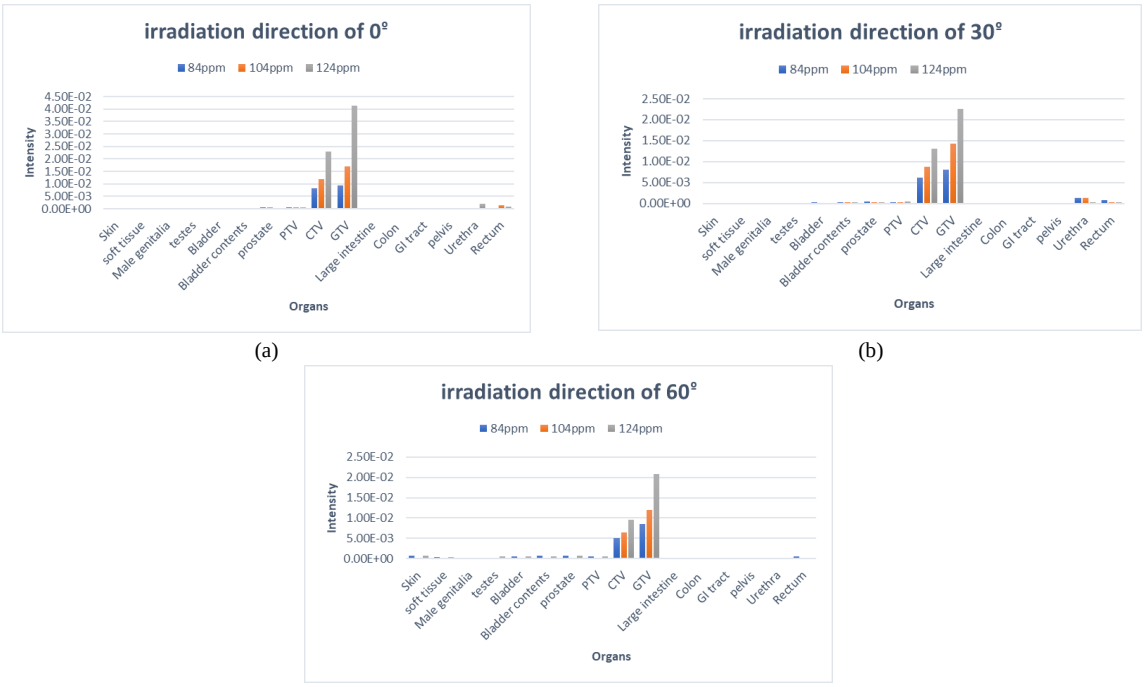

Figure 7. Total dose rate for each OAR from the irradiation direction of (a) 0°, (b) 30°, (c) 60°

Figures 7a-c present the total absorbed dose rate for each organ at risk (OAR) at irradiation angles of 0°, 30°, and 60°. The total dose rate in the gross tumor volume (GTV) increases markedly with boron concentration, consistent with the enhanced probability of the $^{10}B(n, \alpha)^{7}Li$ reaction, which is proportional to the boron atom density ($D_{Total} \propto \Phi\sigma NB$).

For all beam orientations, the gross tumor volume (GTV) received the highest dose rate because of the 10B enrichment ratio of 10 : 5 : 1 (µg/g) among GTV, CTV and normal tissue (International Atomic Energy Agency, 2021). The dose decreased gradually toward surrounding tissues, following the decline in boron concentration and neutron flux intensity. Quantitatively, at 0° irradiation, the GTV dose rate reached 0.0428 Gy/s for 124 µg/g boron, while the bladder and rectum received < 0.005 Gy/s, corresponding to cumulative doses below the 5 Gy safety limit (International Atomic Energy Agency, 2021).

At oblique angles (30° and 60°), the GTV dose rate decreased by ≈ 15–25%, due to increased neutron path lenght and lateral scattering, which reduce the neutron flux at depth. This trend demonstrates that beam alignment along the central axis (0°) maximizes dose delivery efficiency while minimizing irradiation to non-target tissues.

Table 5. Summary of Calculated Dose Rates and Equivalent Dose at GTV (0°, 124 $\mu g/g$)

Component	Physical Dose Rate (Gy/s)	Weighting Factor (ω)	Equivalent Dose Rate ($Gy-Eq/s$)
Boron	$1.02\ x\ 10^{-2}$	3.8	$3.87\ x\ 10^{-2}$
Proton	$5.12\ x\ 10^{-4}$	3.2	$1.64\ x\ 10^{-3}$
Neutron	$6.25\ x\ 10^{-4}$	3.2	$2.00\ x\ 10^{-3}$
Gamma	$4.50\ x\ 10^{-4}$	1.0	$4.50\ x\ 10^{-3}$
Total	$1.18\ x\ 10^{-2}\ (Gy/s)$		$4.15\ x\ 10^{-2}\ (Gy-Eq/s)$

Note: With a total dose rate of $4.15\ x\ 10^{-2}\ (Gy-Eq/s)$, the required irradiation time to achieve the minimum therapeutic dose of 76 $Gy-Eq$ is approximately 30.59 minutes.

3.3 Irradiation Time

The irradiation time required to deliver the prescribed therapeutic dose depends on the total absorbed dose rate. Figure 8 illustrates the relationship between ^{10}B concentration and irradiation time for irradiation angles of 0°, 30°, and 60°.

The results show that increasing boron concentration significantly reduces irradiation time across all configurations. This is consistent with the principle that the total dose rate D_{Total} increases with boron atom density (NB), as the reaction rate $R=\Phi\sigma NB$ of the $^{1}B(n,\alpha)^{7}Li$ process becomes higher. Consequently, the required exposure time $t = D_{target}/D_{Total}$ decreases proportionally.

Among the three angles, based on the optimal simulation parameters (0° beam angle and 124 µg/g boron concentration), the GTV received a total dose rate of $4.15\ x\ 10^{-2}\ (Gy-Eq/s)$. Consequently, to reach the prescribed therapeutic dose of 76 $Gy-Eq$ for the intermediate-risk group, the total irradiation duration was determined to be 30.59 minutes.

This duration falls within the clinically acceptable range of 20–60 minutes for accelerator-based BNCT systems, confirming the feasibility of the proposed treatment configuration (International Atomic Energy Agency, 2021; Suzuki et al., 2014), confirming the feasibility of the modeled configuration.

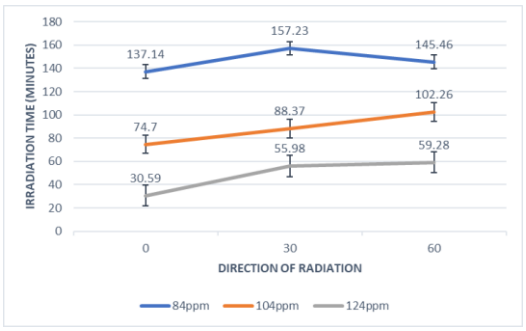

Figure 7. Irradiation Time Graph at angles 0˚, 30°, 60°

3.4 Equivalent Dose to Organs at Risk (OARs)

Figures 9 a-c illustrate the equivalent dose received by each organ at risk (OAR) for irradiation angles of 0°, 30°, and 60°. The gross tumor volume (GTV) consistently received the highest equivalent dose, reaching approximately 76 Gy at 124 µg/g boron, while the surrounding organs such as the bladder and rectum received significantly lower doses (5 Gy).

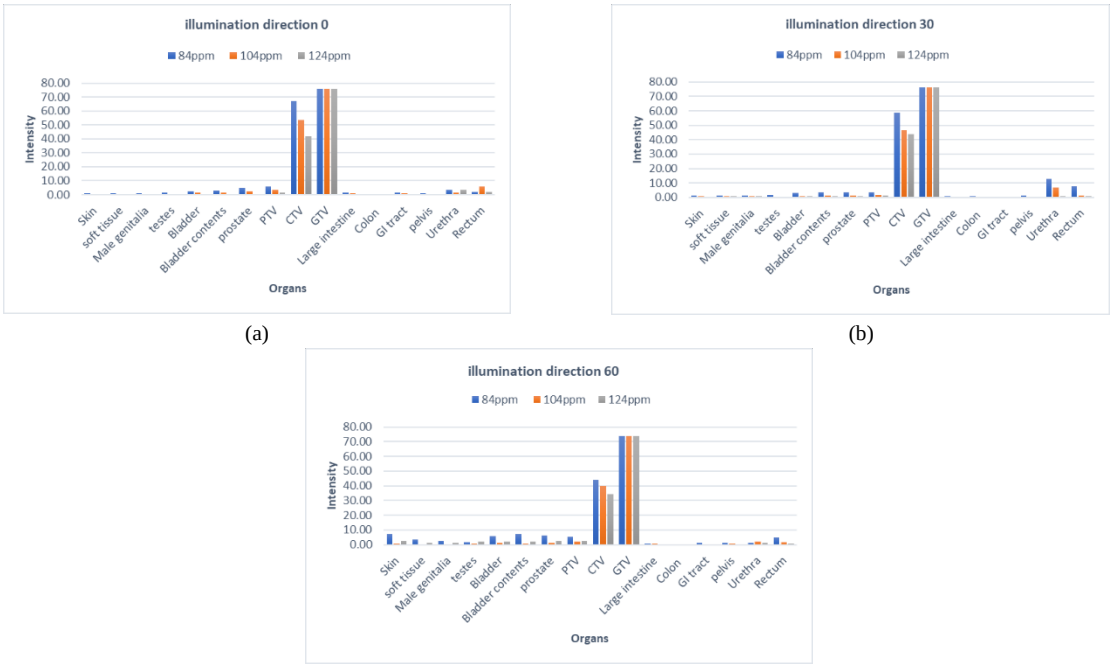

(a) (b)

(c)

Figure 8. Equivalent dose in OAR for radiation direction (a) 0˚, (b) 30˚, (c) 60˚

The ratio of boron concentration between tumor and normal tissue was assumed to 10 : 5 : 1, it means normal tissue receives about 10% of the boron concentration in tumor tissue following standard BNCT tissue uptake data (International Atomic Energy Agency, 2021) Within the tumor, boron uptake was distributed as GTV ≈ 100%, CTV ≈ 50%, and PTV ≈ 5% of the tumor concentration, which reflects the expected gradient in boron delivery (Mirzaei et al., 2014).

As boron concentration increased, the equivalent dose to OARs slightly decreased. This trend results from the selective localization of ^{10}B in tumor tissue, causing most neutron capture reactions to occur within the target volume. The emitted α and ^{7}Li particles have a limited range of 5–9 µm, thus confining energy deposition to the tumor region and reducing dose leakage to surrounding OAR.

All OAR doses remained below the clinical tolerance limit of 5 Gy recommended for pelvic organs in BNCT (International Atomic Energy Agency, 2021), confirming the selectivity and safety of the modeled configuration.

3.5 Comparative And Physical Analysis

Based on the simulation results and dose distribution analysis, variations in irradiation direction irradiation direction significantly influence the dose conformity and protection of surrounding organs. The 0° beam orientation exhibited the most symmetric and concentrated dose distribution on the tumor volume, with a steep dose fall-off toward the bladder and rectum. In contrast, irradiation at 30° and 60° produced elongated isodose patterns, indicating lateral neutron scattering and increased penetration path length, which decreased the dose conformity.

The 0° configuration provided the highest overall dose conformity and the most uniform dose coverage across the gross tumor volume (GTV), demonstrating optimal geometric alignment between the neutron beam and the tumor

center. This condition reduced neutron attenuation and allowed a more direct flux incidence on the GTV, resulting in higher absorbed dose rates and more stable irradiation times across boron concentrations.

At oblique irradiation angles, the increased path length of neutrons through normal tissue (following $x = d/\cos\theta$) led to enhanced scattering and reduced effective flux density at the target, which consequently decreased both the total and equivalent doses in the tumor region by approximately 15–25%. This behavior is consistent with previous Monte Carlo studies on BNCT beam orientation (Suzuki et al., 2014; Koivunoro et al., 2019), which reported that beam direction plays a crucial role in determining dose conformity and treatment efficiency.

Physically, the relationship between boron concentration, neutron flux, and absorbed dose rate can be expressed as:

$$\dot{D}_T = \Phi_\sigma N_B E_{\alpha,Li} \quad (5)$$

where Φ is the thermal neutron flux, σ is the microscopic capture cross-section of ^{10}B (3.84×10^{-22} cm²), NB is the boron atom density, and E_(α,Li) represents the total energy released from the $^{10}B(n,\alpha)\,^{7}Li$ reaction (~2.79 MeV). This proportional relationship explains the observed linear increase in dose rate with boron concentration and the corresponding decrease in irradiation time. From a therapeutic standpoint, the optimal configuration (0° irradiation at 124 µg/g boron concentration) achieved the most favorable dose conformity and maintained OAR doses below 5 Gy, fulfilling the IAEA clinical safety guidelines (International Atomic Energy Agency, 2021).

These results are consistent with previous studies (Suzuki et al., 2014; Koivunoro et al., 2019; Barth et al., n.d.) which demonstrated that increased boron concentration and accurate beam alignment enhance treatment efficiency and dose selectivity in BNCT. The equivalent dose to the tumor region obtained in this simulation (~76 Gy at 124 µg/g) falls within the therapeutic range reported by Barth et al. (2018) for clinical BNCT (60–80 Gy-Eq), while doses to surrounding organs remained within the 5 Gy tolerance limit, confirming both the physical reliability and clinical feasibility of the modeled system. These findings highlight that precise beam orientation, optimized boron delivery, and accurate dose modeling play essential roles in improving therapeutic gain and minimizing collateral damage in accelerator-based BNCT applications.

4. Conclusions

Variations in irradiation direction and boron concentration significantly influenced dose conformity, dose rate, and irradiation time in accelerator-based Boron Neutron Capture Therapy (BNCT) for prostate cancer. The 0° beam orientation achieved the highest conformity index and the lowest exposure to organs at risk (OARs), with an equivalent tumor dose of approximately 76 Gy and a total irradiation time of 30.59 minutes. Increasing boron concentration from 84 µg/g to 124 µg/g improved neutron capture efficiency, resulting in higher absorbed dose within the gross tumor volume (GTV) and reduced treatment time, while OAR doses remained below the clinical tolerance limit of 5 Gy.

These findings confirm the physical reliability of PHITS-based Monte Carlo simulations for dose optimization in BNCT and demonstrate that angular configuration plays a critical role in achieving an optimal balance between tumor control and normal tissue protection. These results can serve as a quantitative reference for the development of treatment-planning protocols in accelerator-based BNCT systems, particularly for prostate and other deep-seated malignancies.

5. Recommendations

a) Future work should include patient-specific anatomical modeling using CT or MRI data to improve dose accuracy and clinical applicability.
b) Further optimization of beam energy spectra and boron compound pharmacokinetics is recommended to enhance treatment selectivity.
c) Experimental validation using physical phantoms or benchmark data is necessary to confirm the Monte Carlo results and support clinical translation.

Overall, the simulation results contribute to the ongoing development of accelerator-based BNCT by providing quantitative insights into the influence of beam orientation and boron concentration on dose distribution, which may serve as a foundation for future clinical treatment planning and system optimization.

Acknowledgment

The authors would like to express our deepest gratitude and highest appreciation to the Physics Study Program, Faculty of Mathematics and Natural Sciences, National Defense University, as well as the National Research and Innovation Agency, Center for Safety, Metrology, and Nuclear Quality Technology Research, Ionizing Radiation Dosimetry Research Group, for all forms of assistance and support provided during this research process.

Author Contribution

This research received significant contributions from Muhammad Nashrun Basyaruddin, Raditya Faradina Pratiwi , Yohannes Sardjono, Gede Sutrisna Wijaya, Isman Mulyadi Triatmoko, Fendinugroho, Nunung Nuraeni, and Heru Prasetio. The other authors participated by reading and approving the final version of the manuscript.

6. Bibliography

Ardana, I. M., & Sardjono, Y. (2017). Optimization of a neutron beam shaping assembly design for BNCT and its dosimetry simulation based on MCNPX. *Jurnal Teknologi Reaktor Nuklir Tri Dasa Mega, 19*(3), 121. https://doi.org/10.17146/tdm.2017.19.3.3582

Arigbede, O., Buxbaum, S. G., Falzarano, S., & Rhie, S. K. (2024). Global disparities in prostate cancer burden: An analysis of the GLOBOCAN 2020 database. *Cancer Epidemiology, Biomarkers & Prevention, 33*(9 Suppl), C001–C001. https://doi.org/10.1158/1538-7755.DISP24-C001

Barth, R. F., Coderre, J. A., Vicente, M. G., & Blue, T. E. (2005). Boron neutron capture therapy of cancer: Current status and future prospects. *Clinical Cancer Research, 11*(11), 3987–4002.

Bolland, W. (2008). Prostate cancer. *InnovAiT: Education and Inspiration for General Practice, 1*(9), 642–650. https://doi.org/10.1093/innovait/inn114

Feuvret, L., Noël, G., Mazeron, J. J., & Bey, P. (2006). Conformity index: A review. *International Journal of Radiation Oncology Biology Physics, 64*(2), 333–342. https://doi.org/10.1016/j.ijrobp.2005.09.028

Fukuda, H. (2021). Boron neutron capture therapy for cutaneous malignant melanoma using BPA. *Cells*. https://doi.org/10.3390/cells10112881

International Agency for Research on Cancer. (2022). *Indonesia source: GLOBOCAN 2022 (The Global Cancer Observatory)*. https://gco.iarc.fr/today/data/factsheets/populations/360-indonesia-fact-sheets.pdf

International Atomic Energy Agency. (2001). *Current status of neutron capture therapy*. https://www.iaea.org/publications/6134/current-status-of-neutron-capture-therapy

Jagt, T. Z., Janssen, T. M., & Sonke, J. J. (2024). Evaluating the effect of higher Monte Carlo statistical uncertainties on accumulated doses after daily adaptive fractionated radiotherapy in prostate cancer. *Physics and Imaging in Radiation Oncology, 32*. https://doi.org/10.1016/j.phro.2024.100636

Jain, M. A., & Sapra, A. (2020). Prostate cancer screening. *StatPearls*. https://pubmed.ncbi.nlm.nih.gov/32310541/

Jin, W. H., Seldon, C., Butkus, M., Sauerwein, W., & Giap, H. B. (2022). A review of boron neutron capture therapy: Its history and current challenges. *International Journal of Particle Therapy*. https://doi.org/10.14338/IJPT-22-00002.1

Koivunoro, H., Kankaanranta, L., Seppälä, T., Haapaniemi, A., Mäkitie, A., & Joensuu, H. (2019). Boron neutron capture therapy for locally recurrent head and neck squamous cell carcinoma: An analysis of dose response and survival. *Radiotherapy and Oncology, 137*, 153–158. https://doi.org/10.1016/j.radonc.2019.04.033

Krstic, D., Markovic, V. M., Jovanovic, Z., Milenkovic, B., Nikezic, D., & Atanackovic, J. (2014). Monte Carlo calculations of lung dose in ORNL phantom for boron neutron capture therapy. *Radiation Protection Dosimetry, 161*(1–4), 269–273. https://doi.org/10.1093/rpd/nct365

Kumada, H., Sakae, T., & Sakurai, H. (2023). Current development status of accelerator-based neutron source for boron neutron capture therapy. *EPJ Techniques and Instrumentation, 10*(1). https://doi.org/10.1140/epjti/s40485-023-00105-5

Lee, C. H., Akin-Olugbade, O., & Kirschenbaum, A. (2011). Overview of prostate anatomy, histology, and pathology. *Endocrinology and Metabolism Clinics of North America*. https://doi.org/10.1016/j.ecl.2011.05.012

Li, G., Jiang, W., Zhang, L., Chen, W., & Li, Q. (2021). Design of beam shaping assemblies for accelerator-based BNCT with multi-terminals. *Frontiers in Public Health, 9*. https://doi.org/10.3389/fpubh.2021.642561

Lu, L., An, S., Guan, F., Wang, Z., & Zhao, Y. (2023). Performance research and optimization of beam shaping assembly used for BNCT based on cyclotron. *IEEE Nuclear Science Symposium Conference Proceedings*. https://doi.org/10.1109/NSSMICRTSD49126.2023.10338497

Meher, N., et al. (2021). Synthesis and preliminary biological assessment of carborane-loaded theranostic nanoparticles to target prostate-specific membrane antigen. *ACS Applied Materials & Interfaces, 13*(46), 54739–54752. https://doi.org/10.1021/acsami.1c16383

Mirzaei, D., Miri-Hakimabad, H., & Rafat-Motavalli, L. (2014). Depth dose evaluation for prostate cancer treatment using boron neutron capture therapy. *Journal of Radioanalytical and Nuclear Chemistry, 302*(3), 1095–1101. https://doi.org/10.1007/s10967-014-3397-2

Nakamura, R., Hino, M., Tanaka, H., Kuriyama, Y., & Iwashita, Y. (2022). Conceptual design of a target station using a 30-MeV cyclotron accelerator for BNCT study. *Nuclear Instruments and Methods in Physics Research Section A, 1042*, 167425. https://doi.org/10.1016/j.nima.2022.167425

Ogawa, T., et al. (2024). Overview of PHITS ver. 3.34 with particular focus on track-structure calculation. *EPJ Nuclear Sciences & Technologies, 10*, 13. https://doi.org/10.1051/epjn/2024012

Panebianco, V., et al. (2018). An update of pitfalls in prostate mpMRI: A practical approach through the lens of PI-RADS v2 guidelines. *Insights into Imaging*. https://doi.org/10.1007/s13244-017-0578-x

Purohit, M., & Kumar, M. (2022). Boron neutron capture therapy: History and recent advances. *Materials Today: Proceedings*. https://doi.org/10.1016/j.matpr.2022.12.181

Schwint, A. E., et al. (2020). Clinical veterinary boron neutron capture therapy studies in dogs with head and neck cancer. *Biology, 9*(10). https://doi.org/10.3390/biology9100327

Sung, H., Ferlay, J., Siegel, R. L., Laversanne, M., Soerjomataram, I., Jemal, A., & Bray, F. (2021). Global cancer statistics 2020: GLOBOCAN estimates of incidence and mortality worldwide for 36 cancers in 185 countries. *CA: A Cancer Journal for Clinicians, 71*(3), 209–249. https://doi.org/10.3322/caac.21660

Suzuki, M., et al. (2014). Boron neutron capture therapy outcomes for advanced or recurrent head and neck cancer. *Journal of Radiation Research*. https://doi.org/10.1093/jrr/rrt098

Wang, S., Zhang, Z., Miao, L., & Li, Y. (2022). Boron neutron capture therapy: Current status and challenges. *Frontiers in Oncology*. https://doi.org/10.3389/fonc.2022.788770

Yeom, Y. S., et al. (2019). Computation speeds and memory requirements of mesh-type ICRP reference computational phantoms in Geant4, MCNP6, and PHITS. *Health Physics, 116*(5).

Zhang, Y. N., et al. (2022). Gross tumor volume delineation in primary prostate cancer on 18F-PSMA-1007 PET/MRI and 68Ga-PSMA-11 PET/MRI. *Cancer Imaging, 22*(1). https://doi.org/10.1186/s40644-022-00475-1